ChemComm

Cite this: *Chem. Commun.*, 2012, **48**, 4998–5000

www.rsc.org/chemcomm

COMMUNICATION

Alkali earth metal (Ca, Sr, Ba) based thermostable metal–organic frameworks (MOFs) for proton conduction†

Tanay Kundu, Subash Chandra Sahoo and Rahul Banerjee*

Received 15th February 2012, Accepted 23rd March 2012
DOI: 10.1039/c2cc31135f

Three new alkaline earth metal based MOFs have been synthesized by using 4,4′-sulfobisbenzoic acid (SBBA) and alkaline earth metal salts M(NO_3)$_2$, M = Ca, Sr, Ba. These MOFs exhibit interesting structural diversity, variable chemical stability as well as proton conductivity.

Design of proton conductors is enormously important in proton exchange membrane based fuel cells (PEMFCs). Currently, Nafion is used as a proton conductor in PEMFCs,[1] which suffers from dehydration followed by very low proton conductivity above 80 °C. Several attempts have been made to design inorganic, organic and hybrid materials[2] that will show proton conduction at temperatures higher than 80 °C. MOFs, being a crystalline class of compounds, with diverse topological architecture have the potential to overcome the limitation of Nafion based membranes in terms of their proton conductivity. Surprisingly, MOFs as proton conductors have not been explored as widely as applications like gas sorption,[3] catalysis,[4] and magnetism.[5] Unlike classical porous materials, MOFs provide the opportunity for highly tunable architecture as well as control over hydrophobicity or hydrophilicity *via* judicious choice of organic linkers. Till date very few proton conducting MOFs have been reported where the lattice backbone, guest molecules[6] in anhydrous medium, or already present water chains and clusters inside the framework[7] act as a proton carrier. However, the effect of metal ion substitution on proton conducting MOFs is still unexplored. Hence, there remains a necessity to understand the judicious choice of metal nodes to design organic–inorganic hybrid materials for proton conduction.

Herein, we present three new two dimensional MOFs, namely Ca-SBBA, Sr-SBBA and Ba-SBBA, constructed from alkaline earth metals *i.e.* Ca(II), Sr(II) and Ba(II) as metal nodes and 4,4′-sulfobisbenzoic acid (SBBA) as an organic linker. The polysulfone backbone in polymers is well known for high proton conductivity applications.[8] SBBA also possesses a similar sulfone functionality, apart from the carboxylate functionalities, which motivated us to choose SBBA as an effective candidate to design proton conducting MOFs. Interestingly, the structures are completely different from each other although they bear the same ligand and the same group of metal atoms. All these three MOFs have thermal stability up to 500 °C, with a crystalline phase change above 100 °C. Most interestingly, they exhibit noticeable difference in proton conductivity under hydrous conditions. Ca-SBBA shows proton conductivity of 8.6×10^{-6} S cm^{-1}, whereas Sr-SBBA shows proton conductivity of 4.4×10^{-5} S cm^{-1} at 298 K under 98% humidity. Ba-SBBA does not show any proton conductivity under similar conditions. To the best of our knowledge this the first report of a systematic study of architectural diversity and proton conduction ability of the alkali earth metals.

Ca-SBBA can be synthesized by mixing equimolar amounts of Ca(NO_3)$_2$·4H_2O (0.2 mmol) and SBBA (0.2 mmol) in *N*,*N*′-dimethylformamide (2 mL) and heating subsequently at 100 °C for 48 h. Sr-SBBA can be synthesized in a similar way, only prolonged heating (96 h) is necessary. For synthesis of Ba-SBBA, *N*,*N*′-diethylformamide serves as a suitable solvent (Section S1 in ESI†). Ca-SBBA and Sr-SBBA are stable in moisture and most common organic solvents (CH_3OH, CH_3CN, C_2H_5OH, THF, dioxane *etc.*), as confirmed by the Powder XRD diffraction (see Fig. S23 and S24 in ESI†). The Ca(II) center adopts an octahedral geometry, with four μ_2 carboxylate oxygens of SBBA at equatorial positions and two DMF molecules at axial positions. These μ_2 carboxylate oxygens connect another Ca(II) and form a one dimensional network[9] which upon interconnection results in a two dimensional sheet like architecture (Fig. 1). These sheets further self-assemble through two C–H···O[10] hydrogen bonds between coordinated and non-coordinated DMF molecules entrapped between two sheets to form the 3D supramolecular architecture (Fig. 1). The crystal structure of Sr-SBBA consists of an unusual pentanuclear metal cluster linked through carboxylate groups of the SBBA ligand, creating three distinct SBUs, where Sr(II) metal centers form either ten coordinated SrO_{10} or eight coordinated SrO_8 polyhedra. Among these three SBUs, SBU-1 consists of one Sr(II) atom coordinated to two μ_1, six μ_2 carboxylate groups. SBU-2 contains one Sr(II) atom coordinated to two μ_1, two μ_2 carboxylate oxygens and two coordinated DMF molecules, whereas SBU-3 consists of one μ_1 formate anion, four μ_2 carboxylate oxygens and two coordinated DMF molecules. The clusters are connected to neighboring clusters *via* four SBBA ligands to form the 2D architecture. In the crystal

---

Physical/Materials Chemistry Division, National Chemical Laboratory, Dr. Homi Bhabha Road, Pune 411008, India.
E-mail: r.banerjee@ncl.res.in; Tel: +91 2025902535

† Electronic supplementary information (ESI) available: Experimental procedures and additional supporting data. CCDC 850219–850221. For ESI and crystallographic data in CIF or other electronic format see DOI: 10.1039/c2cc31135f

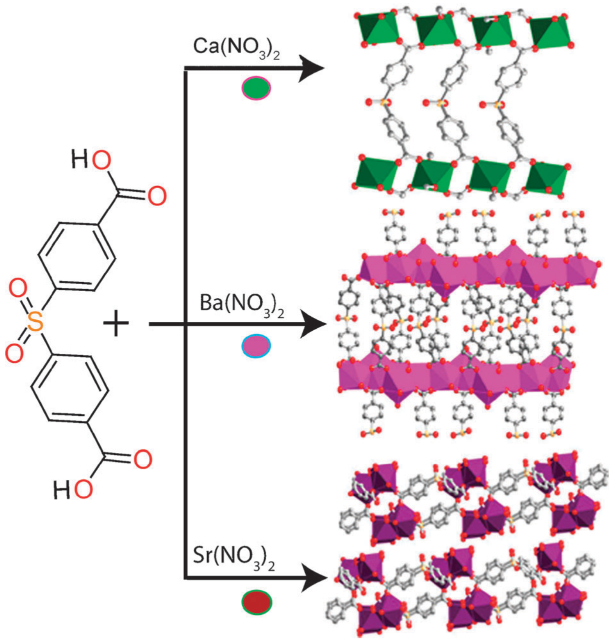

Fig. 1 (a) Schematic representation of architectural diversity of the alkali earth metal (Ca, Sr, Ba) based MOFs showing different binding modes of SBBA as well as different coordination of metals [color code: green: Ca, magenta: Ba, red: O, yellow: S, violet: Sr, black/grey: C].

structure of Ba-SBBA, three types of SBUs are present, where the Ba(II) metal centers create either nine coordinated BaO_9 polyhedra (SBU-1 and -2) or ten coordinated BaO_{10} polyhedra (SBU-3), SBU-1, -2, -3 of Ba-SBBA consist of two μ_2 carboxylate and three, four and three μ_2 carboxylate functionalities, respectively. These μ_2 carboxylate groups link two neighboring Ba(II) to form a one dimensional Ba chain along the crystallographic *a* axis. SBBA links these two Ba chains in a zigzag fashion to construct the two dimensional architecture. Interestingly, these three MOFs possess completely different architectures despite containing the same Group II metals of the periodic table, possibly due to diverse metal coordination number (six for Ca, eight and ten for Sr and nine and ten for Ba), different binding modes (μ_2 coordinated carboxylate for Ca whereas μ_3 coordinated carboxylate for Sr and Ba) and bending angles (113° for Ca, 97° and 104° for Sr and 97° for Ba) of the SBBA ligand (see Section S3 in ESI† for crystallographic details of Ca-SBBA, Sr-SBBA and Ba-SBBA).

In order to confirm the phase purity of the bulk materials, powder X-ray diffraction (PXRD) experiments were carried out on Ca-SBBA, Sr-SBBA and Ba-SBBA. All major peaks of experimental PXRD of as synthesized MOFs match well with simulated PXRDs, indicating their crystalline phase purity (see Fig. S20–S22 in ESI†). The architectural rigidity, as well as the thermal stability of all three MOFs, was well reflected from their VTPXRD data (see Fig. S30–S32 in ESI†). The VTPXRD patterns of Ca-SBBA, Sr-SBBA and Ba-SBBA reveal that the frameworks undergo irreversible structural transformation to a different crystalline phase above 100 °C, due to loss of occluded solvent molecules, and all these transformed crystalline phases are stable up to 500 °C. However, the transformed phases hold the same metal–ligand connectivity like the as-synthesized MOFs, as confirmed from IR spectroscopic comparison of the as-synthesized and heated materials at 500 °C of Ca-SBBA, Sr-SBBA and Ba-SBBA (see Sections S4, S8 and S12 in ESI†). The DSC patterns are also in accordance with the VTPXRD data, which shows that all these materials undergo irreversible phase transformation above 100 °C, confirmed by an endothermic peak at ~100 °C. High bond energy between the alkali earth metal and the carboxylate moiety is primarily responsible of this high thermal stability. The TGA trace for as synthesized materials showed a weight-loss step (25–200 °C) which signifies escape of floating and coordinated DMF or DEF molecules. The long plateau from 200 °C to 500 °C represents the thermal stability of these MOFs, followed by a weight loss step due to the decomposition of the framework. We have also performed the TGA analysis of the humidified Ca-SBBA and Sr-SBBA, which shows less weight loss than as-synthesized MOFs, which justifies the fact that high molecular weight DMF molecules are replaced by low molecular weight water molecules (see Fig. S36 and S37 in ESI†). Ca-SBBA and Sr-SBBA have good chemical stability under humidified conditions, which is evident from well matched simulated and humidified samples PXRD patterns collected after 24 and 48 h of humidification under 98% humidity (see Fig. S25 and S26 in ESI†). However, Ba-SBBA loses its crystallinity and phase purity upon humidification and converts to an amorphous material (see Fig. S27 in ESI†).

Ion conduction in solid state materials[11] occurs intrinsically through the material or *via* some carrier mediated pathway (*e.g.* H_2O, H_3O^+, HO^- *etc.*). Proton conduction in Ca-SBBA and Sr-SBBA was measured by a quasi-four-probe method, with a Solartron 1287 Electrochemical Interface with a 1255B frequency response analyzer. Interestingly, the as synthesized compounds do not show any proton conductivity. Only after humidification for 24 h they start showing proton conduction, which eventually confirms the role of water as a proton carrier. Presumably, the water molecules are absorbed within the crystal by strong hydrogen bonding with the carboxylate bound metal clusters, highly electronegative sulfone groups and the non-coordinated DMF molecules, which facilitates the proton conduction. The proton conductivity value was measured for Ca-SBBA as 8.58×10^{-6} S cm^{-1}, whereas Sr-SBBA shows higher proton conductivity of 4.4×10^{-5} S cm^{-1}, respectively, at ambient temperature (298 K) under 98% relative humidity (RH) (Fig. 2a and 3a). The conductivities were determined from the semicircles in the Nyquist plots, as shown in Fig. 2 and 3. These values are highly humidity-dependent and dropped to 2.87×10^{-7} S cm^{-1}, 3.47×10^{-6} S cm^{-1} at 60% RH, respectively, for Ca-SBBA and Sr-SBBA at 298 K. Ca-SBBA and Sr-SBBA show proton conductivity up to 318 K and 313 K, respectively. The proton conductivity value of Ca-SBBA is comparable with that of MIL-53 based MOFs (10^{-6}–10^{-7} S cm^{-1})[12] whereas the proton conductivity value of Sr-SBBA is comparable with those of PCMOF-3 (3.5×10^{-5} S cm^{-1})[11e] and Zn(l-L$_{Cl}$)(Cl)(H_2O)$_2$ (4.45×10^{-5} S cm^{-1}).[11f] Low temperature proton conductivity measurement reveals the activation energy of 0.23 eV and 0.56 eV for Ca-SBBA and Sr-SBBA, respectively. Hence the proton conduction for Ca-SBBA follows the Grotthuss proton hopping mechanism.[12] However, higher activation energy for Sr-SBBA indicates the Grotthuss mechanism along with some other processes such as direct diffusion of additional protons

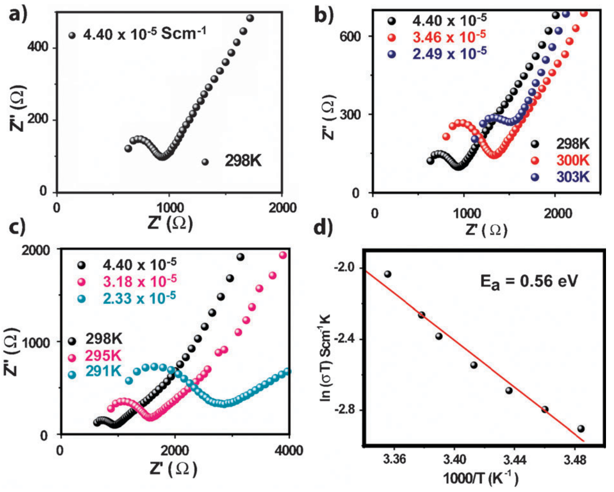

Fig. 2 (a) The Nyquist plot for proton conductivity of Sr-SBBA at 298 K in 98% humidity. (b) Proton conductivity plots of Sr-SBBA at higher temperatures showing decreasing trend of proton conductivity. (c) Proton conductivity plots of Sr-SBBA at lower temperatures showing decrease in proton conductivity. (d) Arrhenius plot of activation energy for Sr-SBBA showing activation energy value of 0.56 eV.

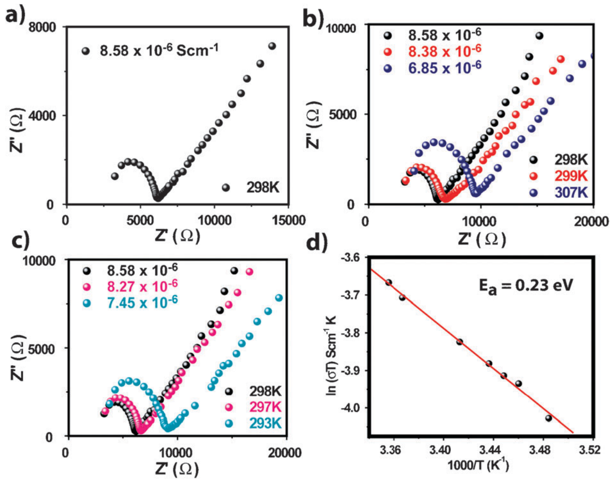

Fig. 3 (a) The Nyquist plot for proton conductivity of Ca-SBBA at 298 K in 98% humidity. (b) Proton conductivity plots of Ca-SBBA at higher temperatures showing decrease in proton conductivity. (c) Proton conductivity plots of Ca-SBBA at lower temperatures showing decrease in proton conductivity following Grotthuss proton hopping mechanism. (d) Arrhenius plot of activation energy for Ca-SBBA showing activation energy value of 0.23 eV.

with water molecules or DMF molecules (vehicle mechanism).[13] The fact that Sr-SBBA exhibits higher proton conduction than Ca-SBBA despite the large E_a (0.56 eV for Sr-SBBA whereas 0.23 eV for Ca-SBBA) is indicative of a high carrier concentration, originating from the combination of metal clusters, coordinated and non-coordinated solvent molecules. The structural stability upon humidification was justified by well matched PXRD patterns of Ca-SBBA and Sr-SBBA before and after the proton conduction experiment (see Fig. S28 and S29 in ESI†). However, Ba-SBBA fails to show any conducting property due to phase change and loss of crystallinity upon humidification. Thus, these three alkali earth metal based MOFs exhibit significant difference in proton conductivity owing to their structural variation as well as physico-chemical properties.

In conclusion, we have successfully synthesized three new MOFs using alkali earth metal salts and 4,4′-sulfobisbenzoic acid. These three MOFs exhibit interesting structural variation and distinct binding motifs. Most interestingly, these three MOFs show significant difference in their proton conducting ability. This study may motivate researchers to engage in detailed study and systematic exploration of proton conduction in thermostable MOFs of a less explored group of metals to compete with Nafion and zeolite based materials for practical applications.

Notes and references

1 K. A. Mauritz and R. B. Moore, *Chem. Rev.*, 2004, **104**, 4535.

2 (*a*) B. C. Steele and A. Heinzel, *Nature*, 2001, **414**, 345; (*b*) B. C. Wood and N. Marzari, *Phys. Rev. B*, 2007, **76**, 134301; (*c*) K. D. Kreuer, S. J. Paddison, E. Spohr and M. Schuster, *Chem. Rev.*, 2004, **104**, 4637; (*d*) M. A. Hickner, H. Ghassemi, Y. S. Kim, B. R. Einsla and J. E. McGrath, *Chem. Rev.*, 2004, **104**, 4587.

3 (*a*) H. K. Chae, D. Y. Siberio-Perez, J. Kim, Y. Go, M. Eddaoudi, A. J. Matzger, M. O'Keeffe and O. M. Yaghi, *Nature*, 2004, **427**, 523; (*b*) X. Zhao, B. Xiao, J. A. Fletcher, K. M. Thomas, D. Bradshaw and M. J. Rosseinsky, *Science*, 2004, **306**, 1012; (*c*) J. L. Atwood, L. J. Barbour and A. Jerga, *Science*, 2002, **296**, 2367; (*d*) S. Han, Z. Ma, Y. Wei, V. Ch. Kravtsov, B. S. Luisi, I. Kulaots and B. Moulton, *CrystEngComm*, 2011, **13**, 4838; (*e*) G. Seeber, G. J. T. Cooper, G. N. Newton, M. H. Rosnes, D.-L. Long, B. M. Kariuki, P. Kögerler and L. Cronin, *Chem. Sci.*, 2010, **1**, 62; (*f*) M. Kim, J. F. Cahill, Y. Su, K. A. Prather and S. M. Cohen, *Chem. Sci.*, 2012, **3**, 126.

4 (*a*) J. S. Seo, D. Whang, H. Lee, S. I. Jun, J. Oh, Y. J. Jeon and K. Kim, *Nature*, 2000, **404**, 982; (*b*) C. Wang, M. Zheng and W. Lin, *J. Phys. Chem. Lett.*, 2011, **2**, 1701.

5 (*a*) M. Kurmoo, *Chem. Soc. Rev.*, 2009, **38**, 1353; (*b*) T. Shiga, H. Okawa, S. Kitagawa and M. Ohba, *J. Am. Chem. Soc.*, 2006, **128**, 16426.

6 (*a*) S. Bureekaew, S. Horike, M. Higuchi, M. Mizuno, T. Kawamura, D. Tanaka, N. Yanai and S. Kitagawa, *Nat. Mater.*, 2009, **8**, 831; (*b*) J. A. Hurd, R. Vaidhyanathan, V. Thangadurai, C. I. Ratcliffe, I. M. Moudra-kovski and G. K. H. Shimizu, *Nat. Chem.*, 2009, **1**, 705.

7 (*a*) M. Yoon, K. Suh, H. Kim, Y. Kim, N. Selvapalam and K. Kim, *Angew. Chem., Int. Ed.*, 2011, **50**, 7870; (*b*) Y. Nagao, M. Fujishima, R. Ikeda, S. Kanda and H. Kitagawa, *Synth. Met.*, 2003, **133**, 43.

8 (*a*) R. Nolte, K. Ledjeff, M. Bauerb and R. Mtilhaupt, *J. Membr. Sci.*, 1993, **83**, 211; (*b*) M. A. Hickner, H. Ghassemi, Y. S. Kim, B. R. Einsla and J. E. McGrath, *Chem. Rev.*, 2004, **104**, 4587.

9 (*a*) X.-L. Chen, L. Gou, H.-M. Hu, F. Fu, Z.-X. Han, H.-M. Shu, M.-L. Yang, G.-L. Xue and C.-Q. Du, *Eur. J. Inorg. Chem.*, 2008, 239; (*b*) F.-Y. Lian, F.-L. Jiang, D.-Q. Yuan, J.-T. Chen, M.-Y. Wu and M.-C. Hong, *CrystEngComm*, 2008, **10**, 905.

10 G. R. Desiraju, *Acc. Chem. Res.*, 2002, **35**, 565.

11 (*a*) J. M. Taylor, R. K. Mah, I. L. Moudrakovski, C. I. Ratcliffe, R. Vaidhyanathan and G. K. H. Shimizu, *J. Am. Chem. Soc.*, 2010, **132**, 14055; (*b*) K. D. Kreuer, *Annu. Rev. Mater. Res.*, 2003, **33**, 333; (*c*) M. F. H. Schuster, W. H. Meyer, M. Schuster and K. D. Kreuer, *Chem. Mater.*, 2004, **16**, 329; (*d*) H. Okawa, A. Shigematsu, M. Sadakiyo, T. Miyagawa, K. Yoneda, M. Ohba and H. Kitagawa, *J. Am. Chem. Soc.*, 2009, **131**, 13516; (*e*) A. Shigematsu, T. Yamada and H. Kitagawa, *J. Am. Chem. Soc.*, 2011, **133**, 2034; (*f*) S. C. Sahoo, T. Kundu and R. Banerjee, *J. Am. Chem. Soc.*, 2011, **133**, 17950.

12 (*a*) S. l. Cukierman, *Biochim. Biophys. Acta, Bioenerg.*, 2006, **1757**, 876; (*b*) Proton Conductors: Solids, Membranes and Gels—Materials and Devices, in *Chemistry of Solid State Materials*, P. Colomban, Cambridge University Press, Cambridge, U.K., 1992, vol. 2.

13 (*a*) K. D. Kreuer, A. Rabenau and W. Weppner, *Angew. Chem., Int. Ed. Engl.*, 1982, **21**, 208; (*b*) M. Sadakiyo, T. Yamada and H. Kitagawa, *J. Am. Chem. Soc.*, 2009, **131**, 9906.